Ilorin Journal of Science
Volume 11, Number 1, 2024, pp. 52 – 73 (Printed in Nigeria)
ISSN: 2408 – 4840 © 2023 Faculty of Physical Sciences, University of Ilorin
https://doi.org/10.54908/iljs.2024.11.01.004

ILORIN
JOURNAL OF SCEINCE

ILJS-24- 015

Adsorption of Bromocresol Green Dye on Onion Skin-based Molecularly Imprinted Polymers: Kinetics, Equilibrium, Thermodynamics Studies and DFT Simulation

Awokoya*, K. N., Oninla, V.O., Ohenhen, V., Adelani, A.O., Odulaja, T.T., Onososen, D.A., Olowo, A.O., and Fakola, E.G.

Department of Chemistry, Obafemi Awolowo University, Ile-Ife, 220007, Nigeria

Abstract

This research focuses on the sequestration of Bromocresol green dye (BCGD), an anionic dye, from aqueous medium using onion skin-based molecularly imprinted polymer (OSMIP). The OSMIP was prepared using distilled water as porogen, BCGD as template, divinyl benzene as crosslinker, styrene as functional monomer, and benzoyl peroxide as initiator; while with the non-imprinted analogue (OSNIP) was similarly prepared, but with the exclusion of BCGD. The imprinted polymers were characterized by scanning electron microscopy coupled with energy dispersive x-ray (SEM-EDX), Fourier-transform infrared spectroscopy (FTIR), X-ray diffractometry (XRD) and Thermogravimetry analysis (TGA). The characterization results indicated a successful cavity imprinting and higher thermal stability of OSMIP when compared with OSNIP. The integrity of the polymer material was also observed to be maintained. Batch experimental method was adopted for the adsorption process. OSMIP demonstrated a significantly higher BCGD removal efficiency, compared to OSNIP, possibly due to the imprinted cavities on the polymer. A dye removal efficiency of 99.8% was attained at an initial dye concentration of 25 mg L^{-1} and pH 6 for OSMIP. Kinetic data were well described by the pseudo-second-order model, while equilibrium data best fitted the Langmuir isotherm. Maximum adsorption capacity of 86.96 mg g^{-1} was obtained. OSMIP reusability study showed appreciable efficiency up to ten consecutive adsorption/desorption cycles, with a minimal loss in efficiency of just 7.4%. The density functional theory analysis provided support for the experimental findings, indicating the high potential of OSMIP in removing organic dyes from real textile wastewater.

Keywords: Onion skin; Imprinted polymer; Adsorption; Anionic dye; Density functional theory

1. Introduction

Over the years, contaminants from agricultural and industrial activity of humans have resulted in the significant environmental concerns (Yang *et al.*, 2020). These contaminants, such as dyes, metals, pharmaceuticals, fertilizers and pesticides can end up in the water bodies and thus pose threat to the health of humans and animals (Wang *et al.*, 2021a). Reports indicate that about 100 tonnes of dyes are yearly released into water bodies (Yagub *et al*., 2014). It has even been established that at concentrations lower than 1 mg/L, these dyes exhibit toxic properties

Corresponding Author: **Awokoya, K. N.**

Email**:** **knawokoya@oauife.edu.ng or knawokoya@gmail.com**

and can have adverse effects on the environment and on human as well (Hai *et al.*, 2007; Amel *et al.,* 2012). For instance, some dyes have been discovered to interfere with the photosynthesis processes of aquatic organisms (Seow *et al.,* 2016). Furthermore, exposure to many of these dyes pose serious hazard to man, including dermatitis, carcinogenic, and mutagenic effects, as well as kidney disease (Fontana *et al.,* 2018; Lellis *et al*., 2019).

Bromocresol green dye (BCGD) is a dye with basic skeleton of triarylmethane that is anionic in nature, having molecular formular of $C_{21}H_{14}Br_4O_5S$ (Awokoya *et al.,* 2024). Generally, they are widely applied mainly in fiber – polyamide and wool – dyeing. They are also known to have diverse applications in medicine, e.g. in the measurement of serum albumin in blood tests. In clinical practice, it is used as a diagnostic technique. In addition, it is also used chiefly as pH indicator in microbiology, as well as in thin layer chromatography (TLC) for the visualization of the components of the reaction mixture whose pKa is below 5.0 in experimental chemistry (Trivedi *et al.,* 1997). Owing to the anionic nature of BCGD and the presence of $-HSO_3$ (sulfonic acid) group (a known group of toxic pollutants) in its structure, the removal of this kind of dye has become very necessary (Lu *et al.,* 2007; Murmu *et al.,* 2018).

Several researchers have investigated biological, physical, chemical and hybrid methods of removing and treatment of dye-containing wastewaters (Holkar *et al.,* 2016). Among these techniques are ion exchange, chemical oxidation, chemical precipitation, reverse osmosis, electro-coagulation, irradiation, membrane filtration, flocculation, photocatalysis, biological treatments and integrated approaches (Banat *et al.,* 1996; Babu *et al.,* 2007; Zaharia *et al*., 2007; Ali *et al.,* 2011; Emembolu *et al.*, 2017; Yadav *et al*., 2021; Okan *et al.*, 2022; Awokoya *et al*., 2024). Notwithstanding the effectiveness of these processes, unfortunately, have certain drawbacks that include high cost of reagents, high energy cost, toxic sludge generation and the need for extensive treatment areas (Nwabanne *et al.,* 2018; Hassan-Ibrahim *et al.,* 2024).

However, adsorption provide several advantages over all the methods mentioned earlier and has proven to be more effective and efficient with regards to cost, design simplicity and acceptability (Kumar *et al.,* 2014; Ogbodu *et al.,* 2015; Matouq *et al*., 2015; Awokoya *et al.*, 2013; 2022). Several adsorbents from agricultural waste, as well as industrial by-products have been reported in the literature by researchers, these include, garlic peel, calcium alginate composite, tea seed shells, cotton, activated carbon, maize cob, chitin, sugarcane bagasse, zeolites, coir pith, chitosan fibres, peat, wood, plum kernels, carbon nanotube etc. but none of these adsorbents are selective (Wang *et al.,* 2021b; Jain *et al*., 2003). Therefore, the objective of this research was to qualitatively develop innovative polymeric adsorbents that are selective towards BCGD by incorporating onion skin into molecularly imprinted polymer (MIP). MIP are synthetic polymers that are prepared with pre-determined selectivity. Precisely, as at today, MIP has been the most versatile and excellent choice adsorbent for removing dyes from complex medium due to its robustness, stability, simplicity of preparation, and specificity. More, importantly, MIPs are highly selective along with durability in harsh chemical conditions, making them desirable adsorbent for addressing environmental pollution (Khajeh *et al.,* 2011; Awokoya *et al.,* 2013). The choice of incorporating onion skin into the MIP was to contribute to a wider understanding of the chemistry of a plant polyphenol called quercetin (about 44% component of onion skin) with functional monomer and template molecule used

in the synthesis of MIP in this study. It has been established in the literature that the total quercetin content in the component of onion skin is substantially higher than in the eatable parts (Mogren, 2006). The novelty of this study resides in the quercetin forming $\pi - \pi$ stacking interaction with styrene functional monomer, BCGD template molecule, and divinyl benzene crosslinking agent, respectively. Furthermore, the unique aspect lies in the application of the developed onion skin molecularly imprinted polymer (OSMIP) as adsorbent for effective removal of BCGD from aqueous medium.

Porous carbon derived from onion skin has been utilized to capture methylparaben in contaminated water by some researchers (Adeola *et al.,* 2023). To the best of our knowledge, no work has been reported on the use of onion skin-based MIP for the sequestration of BCGD from aqueous solution. Furthermore, an extensive material characterization and regeneration of spent OSMIP adsorbent were performed and here reported. Computational energy analysis, using the Density functional theory (DFT) method, was also investigated to know the most suitable functional monomer for the synthesis of the OSMIP.

2. Materials and methods

2.1.Materials and onion skin preparation

Bromocresol green, along with all other chemicals and reagents including divinyl benzene (DVB), styrene (ST), benzoyl peroxide (BPO), acetic acid, and methanol (MeOH), were obtained from Sigma-Aldrich (Steinheim, Germany). All chemicals and reagents were used as purchased. The working solutions were prepared with distilled water from the BASIC/PH4 PURE-HIT STILL system (BHANU Scientific Instruments Company, Bangalore, India). Samples of onion bulbs (*Allium cepa L.*) were obtained from Akinola local market in lle-lfe, and then identified (voucher specimen number: $IFE - 18291$) at the Botany Department, OAU, Ile-Ife, Nigeria. The onion bulbs were sorted, skins (OS) were manually removed and the impurities were taken off the surface of the OS sample by thorough rinsing with water. This was followed by oven drying at 40℃. The dried OS sample was crushed into powder with mortar and pestle and sieved with a laboratory mesh to obtain <0.2 mm particles. It was then encased in a plastic container and stored at room temperature for further analyses.

2.2.Instrumentation

Various analytical techniques were employed in the characterization of the developed polymers. The surface morphology and elemental composition of the OSMIPs were studied using the combination of scanning electron microscopy (SEM) and energy dispersive X-ray spectroscopy EDX (SEM-EDX, Phenom ProX, Thermo Fisher Scientific, USA); X-ray diffraction (XRD) study was performed with Rigaku MiniFlex – 600 X-ray diffractometer (the diffractograms were recorded at 2θ values of 2º-70º), the EDX analysis was carried out to know the composition of the main constituent atoms present in the polymers; to know the functional group embedded in the polymer matrix, Fourier transformed infrared spectrometer (FTIR) was used to obtain FTIR spectra in the 400-4000 cm^{-1} (Nicolet 330 spectrometer,

Thermo Fisher Scientific, USA); while thermogravimetric/differential thermal analysis (TGA/DTA) was carried out using PerkinElmer analyzer, TGA-4000, Waltham, MA, USA to estimate the thermal stability of the polymers.

2.3. Preparation of Onion Skin-incorporated Molecularly Imprinted Polymer (OSMIP)

OSMIP was prepared by bulk polymerization method, with the BCGD as template molecule, following the procedure reported by Awokoya *et al.* (2024). The preparation of the OSMIP was carried out by mixing 1.426 mmol template molecule (BCGD), 5.588 mmol styrene functional monomer (ST), 11.022 mmol crosslinker (DVB) and 0.4 mg of BPO as initiator in a 100-mL standard flask containing 0.3 g of OS powder and 5 ml of porogen (distilled water). Furthermore, the content of the 100-mL standard flask was then put on a magnetic stirrer and stirred continuously overnight for complete dissolution of all solids. The flask was again placed on a thermostatic hot plate set at 70℃ for 37 min for complete polymerization reaction. The light blue-green solid obtained polymer was ground into powder using mortar and pestle. In a similar procedure, corresponding onion skin incorporated non-imprinted polymer (OSNIP) was synthesized as a control adsorbent but in the absence of the BCGD template molecule. The obtained adsorbents (OSMIP and OSNIP) were stored at room temperature in different sealed plastic containers for further characterization.

2.4. Removal of BCGD from synthesized OSMIP

The BCGD template was extracted from OSMIP particles by a continuous washing of the polymer, using a ratio 1:9 (v/v) mixture of acetic acid and methanol, until no trace of BCGD (the template) was detected when analyzed with a UV–Vis spectrophotometer (Shimadzu UV-Vis – 1800 model, Oregon, USA). Subsequently, the OSMIP polymer was filtered to obtain the "template free" polymer and further rinsed with methanol to get rid of the acetic acid. Lastly, the washed OSMIP was dried for 14 h in an open air. The completely washed and dried OSMIP was collected in a plastic container and labelled as "leached OSMIP".

2.5. Batch adsorption of BCGD to OSMIP and OSNIP

A batch experimental study was conducted to investigate the extent of rebinding of BCGD to the OSMIP and OSNIP. This was conducted using a thermostatic shaker with variable speed (GFL, Burgwedel, Germany) for agitation at 200 rpm. OSMIP/OSNIP (50 mg) was added to each of a series of 20 mL solution of 50 mg L^{-1} BCGD placed inside different 100 mL conical flasks. The pH of the solutions ranged from 1 to 9. The temperature of the water bath was set at 27℃ and the flasks with their contents were agitated for 1 h. The influence of other parameters: contact time (5 to 270 min), initial BCGD concentration (5 to 250 mg L^{-1}) and temperature (40 to 70℃) on BCGD removal by the OSMIP/OSNIP were also investigated. The concentrations of BCGD after the rebinding were analyzed by UV–Vis spectrophotometry at a wavelength of 442 nm. In this study, data were obtained in triplicate, and the average was

taken. To validate the desorption and reusability capacities of the OSMIP, 50 mg of OSMIP was weighed into a conical flask containing 50 mg L^{-1} concentration of BCGD solution, and then subjected to ten (10) adsorption-desorption cycles at agitation time of 60 min. The adsorption efficiency (E) and the quantity of dye adsorbed per unit adsorbent (Q_e) were calculated using Equations 1 and 2, respectively.

$$E = \frac{C_o - C_e}{C_O} \times 100\% \quad (1)$$

$$Q_e = \frac{(C_o - C_e)}{m} V \quad (2)$$

where C_O denotes initial BCGD concentration in the solution before adsorption (mgL^{-1}), $and\ C_e$ denotes equilibrium concentration in the solution after adsorption (mgL^{-1}), V (in liters) represents volume of BCGD used, while m denotes mass of OSMIP or OSNIP (g).

2.6. Modeling the process of adsorption (isotherm, kinetics and thermodynamics)

Four different kinetic models were investigated for the determination of the rate of BCGD adsorption onto OSMIP/OSNIP. They are: Weber-Morris (W-M), Elovich, pseudo-first-order (PFO) and pseudo-second-order (PSO) models (Lagergren, 1898; Weber and Morris, 1963; Ho and Mckay 1999; Cheung *et al*. 2000). For isothermal modeling, four models – Dubinin-Radushkevich (D-R), Langmuir, Temkin and Freundlich models (Freundlich, 1907; Langmuir, 1918; Temkin and Pyzhev, 1940; Dubinin *et al*., 1947) – were also applied in the fitting of the experimental data. Thermodynamic quantities – standard enthalpy change (ΔH°), Gibbs free energy change (ΔG°), and standard entropy changes (ΔS°) – were predicted using equations such as $\Delta G° = \Delta H° - T\Delta S°$, the van't Hoff equation ($\ln K_c = \frac{\Delta G°}{R} - \frac{\Delta H°}{RT}$), and $\Delta G° = -RT\ln K_c$. The values of the quantities were determined from the slope and intercept of the linear plot of $\ln K_c$ versus $^1/_T$.

Where T stands for temperature (K). Gas constant, R, is represented by ($8.314\ J\ mol^{-1}K^{-1}$), while the equilibrium constant, K_c, is defined as $\frac{C_a}{C_e}$, where C_a indicates BCGD concentration on the adsorbent (OSMIP/OSNIP) at equilibrium.

2.7. Computational studies

For computational study, a model of the template-monomer pre-polymerization complex was set up. Based on the knowledge of the literature, one template molecule was encircled by five functional monomer molecules. Quantum calculations in this study were conducted using Spartan 14 software. The DFT method using the B3LYP functional and the 6-31G basis set was utilized to optimize geometry and determine the energy levels of the highest occupied molecular orbital (HOMO) and lowest unoccupied molecular orbital (LUMO). The optimized conformations for the functional monomers (styrene and divinyl benzene) and template molecule (bromocresol green) are depicted in Figure 1.

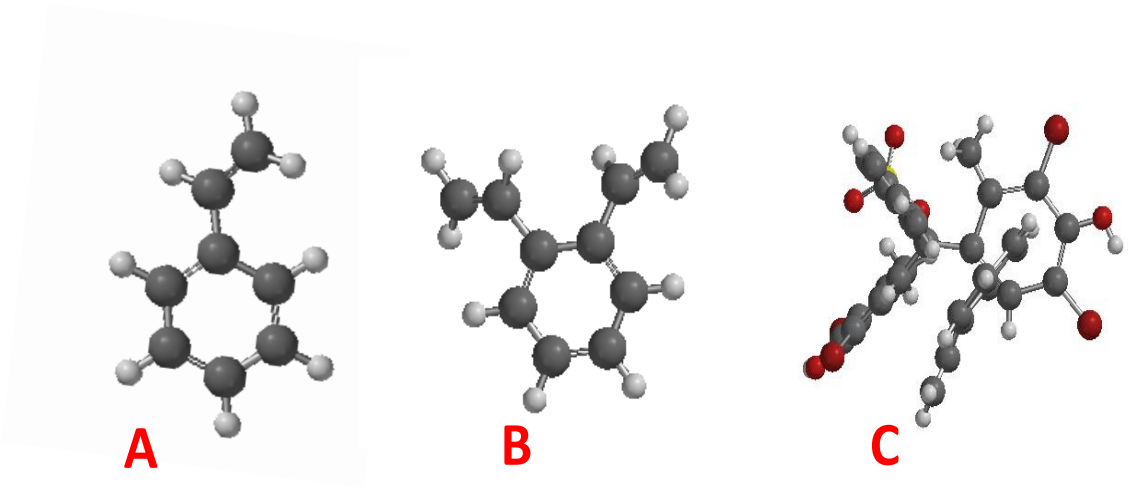

Figure 1: Optimized conformations of styrene (A), divinyl benzene (B) and bromocresol green dye (C)

The binding energies between template and functional monomers were quantified by single-point calculations, utilizing equation (3).

$$\Delta E_{ads} = E_{t\text{-}m} - E_t - \Sigma E_m \quad (3)$$

where E_{t-m} represents interaction energy between BCGD (template) and styrene/divinyl benzene (monomer) molecules, E_t represents the energy of the template molecule, while Em denotes the total energy of the monomer. The quantum parameters (electronic) investigated in this study include the chemical hardness (η), energy gap (ΔE), fractional number of transferred electrons between adsorbate and adsorbent (ΔN) and chemical potential (μ). The quantum parameters, which were later used to predict the adsorption mechanisms, were computed using equations 4, 5, 6, and 7.

$$\eta = \frac{1}{2}(E_{LUMO} - E_{HOMO}) \quad (4)$$

$$\mu = \frac{1}{2}(E_{HOMO} + E_{LUMO}) \quad (5)$$

$$\Delta E = E_{LUMO} - E_{HOMO} \quad (6)$$

$$\Delta N = \frac{\mu_B - \mu_A}{2(\eta_B - \eta_A)} \quad (7)$$

The frontier molecular orbitals energy is represented as E_{LUMO} and E_{HOMO}. Symbols, μ_A and μ_B represent the chemical potentials of the adsorbent and adsorbate, and denote the chemical hardness of the adsorbent and adsorbate as ηA and ηB, respectively.

3. Results and Discussion

3.1. Characterization of OSMIP and OSNIP (SEM-EDX, XRD, FTIR and TGA/DTA)

Figure 2 shows the surface morphological images and the energy dispersive x-ray spectra of the polymers before and after adsorption, as well as that of its non-imprinted counterpart ($OSMIP_{Before}$, $OSMIP_{After}$ and $OSNIP$ particles). In all cases, the images showed that the polymers were strip-shaped and porous on the surface. The $OSMIP_{Before}$ possessed a rougher surface compared to $OSMIP_{After}$ and $OSNIP$ particles, which indicated the presence of cavities (binding sites) on the polymer as a result of the template removal. This is a confirmation of a successful removal of the template from the polymer. After adsorption ($OSMIP_{After}$), the morphology of the polymer revealed relatively smoother structure which may be ascribed to the deposition of the BCGD onto the polymer surface. Surface of the polymer without the template ($OSNIP$) was also smooth and cleaner but with tiny granules. The EDX spectrum revealed that the main constituent of the polymer was carbon (C) with 94.37, 92.25 and 90.94% C for $OSMIP_{Before}$, $OSMIP_{After}$ and $OSNIP$, respectively. Thus, affirming that all the polymer materials are carbonaceous in nature. Figure 4 shows the patterns of x-ray diffraction (XRD) of $OSMIP_{Before}$, $OSMIP_{After}$ and $OSNIP$ adsorbents. Characteristic broad diffraction peaks at $2\theta = 19.96°, 19.72°$ and $19.44°$ were observed for $OSMIP_{Before}$, $OSMIP_{After}$ and $OSNIP$, this could be attributed to the fact that the polymer samples do not exhibit perfect crystallinity. In addition, a small hump in the 2θ range of 9.68º-10.42º was observed in all the three samples. Overall, these results showed that all the samples were amorphous in nature and the imprinting process did not in any way alter the integrity of the polymer materials. Figure 5A depicted the FTIR spectra of the three samples acquired over the range of 500-4000 cm^{-1}. FTIR analysis was conducted to examine the chemical nature of the polymer materials. The only notable change observed in the spectrum of $OSMIP_{After}$, when compared to the spectra of $OSNIP$ and $OSMIP_{Before}$ was the emergence of a peak at 1180.47 cm^{-1}. This peak has been attributed to the $S = O$ of SO_3 group present in sulfonephthalein dyes. The presence of this peak is an indication that BCGD was successfully adsorbed by the $OSMIP_{After}$ adsorbent. The similarities observed in the backbone skeleton structures of the three samples is expected because they all contained same pre-polymerization components (styrene, divinyl benzene, benzoyl peroxide, distilled water etc.). The broad peak in the wavelength range of 3429-3444 cm^{-1} was assigned to $O - H$ stretching of the H_2O molecule used as porogen in the synthesis of the polymers. The peaks at 1454.38 and 1600.97 cm^{-1} were assigned to the symmetric and asymmetric carbonyl stretching vibration of BPO initiator (Prasad *et al.*, 2011). Furthermore, all the spectra had a peak at around 2920.32 cm^{-1} which can be attributed to $C - H$ symmetrical stretching vibrations from CH_2 present in styrene monomer, while the peak at 3024.48 cm^{-1} could be attributable to the $Ar - H$ stretching of styrene, divinyl benzene and BPO.

TGA was employed to evaluate the samples' thermal stability profile. The thermograms of $OSNIP$, $OSMIP_{Before}$, and $OSMIP_{After}$ are shown in Figure 5B. The thermograms revealed that $OSNIP$, $OSMIP_{Before}$, and $OSMIP_{After}$ exhibited a four-step, four-step and three-step degradation process, respectively (three to four steps). For the three samples, the initial thermal decomposition commenced from 25.5℃ and completed at about150℃. The weight loss observed in this initial stage may be attributed to the loss of small moiety like water and/or volatile evaporation (Jaramillo *et al.*, 2016). Generally speaking, the second, third and the

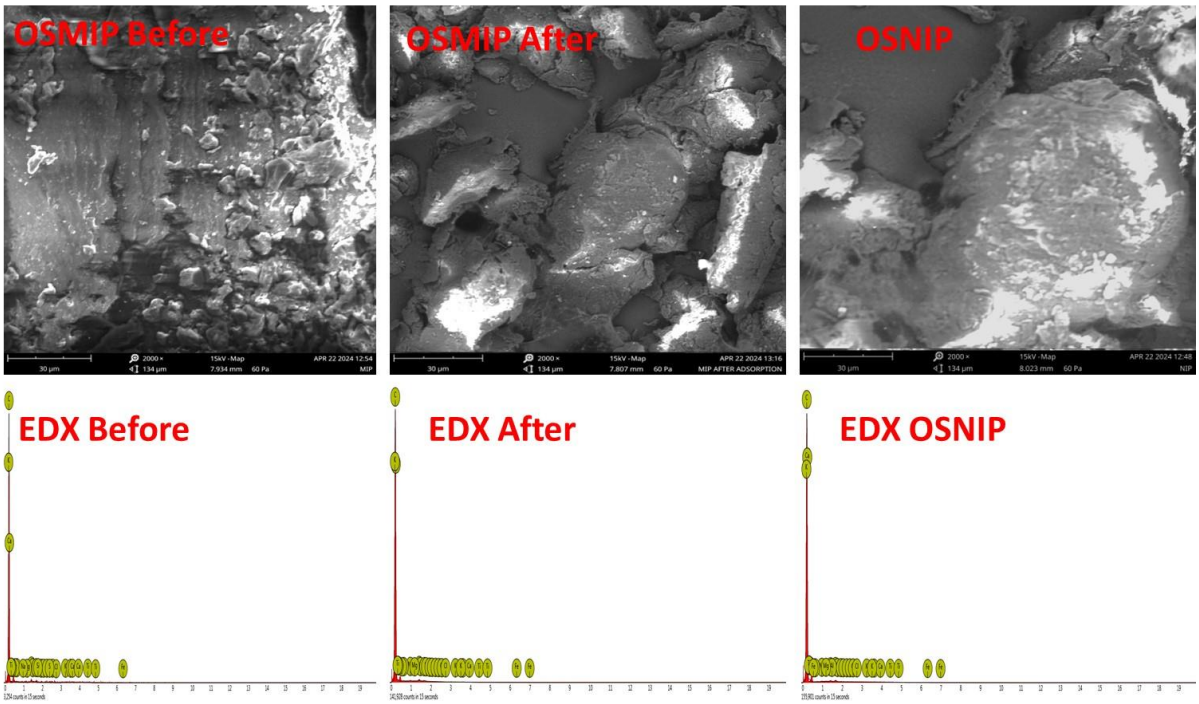

Figure 2: Scanning electron microscopy (SEM) images and energy dispersive X-ray (EDX) spectra of the polymers.

fourth steps belong to the polymer decomposition, i.e. the weight loss at 330-590℃ was related to the polymers. Thus, indicating that the polymers were thermally stable up to about 330℃, had good sturdy properties and can withstand critical working conditions. Additionally, it is relevant to note that $OSMIP_{After}$ was the most stable polymer with a weight loss of 70% at 460℃. This can be explained by the dispersibility of the BCGD molecule on the adsorbent surface after adsorption, which in turn provides greater thermal stability to the $OSMIP_{After}$ material compared to $OSNIP$ and $OSMIP_{Before}$. The interrelated differential thermal analysis (DTA) profile (Figure 3) revealed that the decomposition processes of the polymers are thermally consistent with each other, i.e. they were all endothermic in nature.

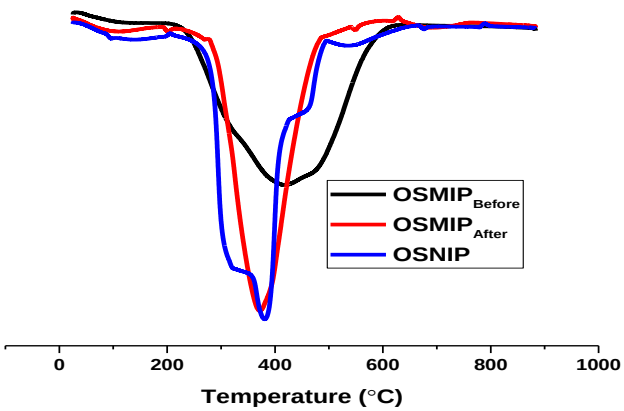

Figure 3: The interrelated differential thermal analysis (DTA) profile for $OSMIP_{Before}$, $OSMIP_{After}$ and OSNIP (Supplementary Figure).

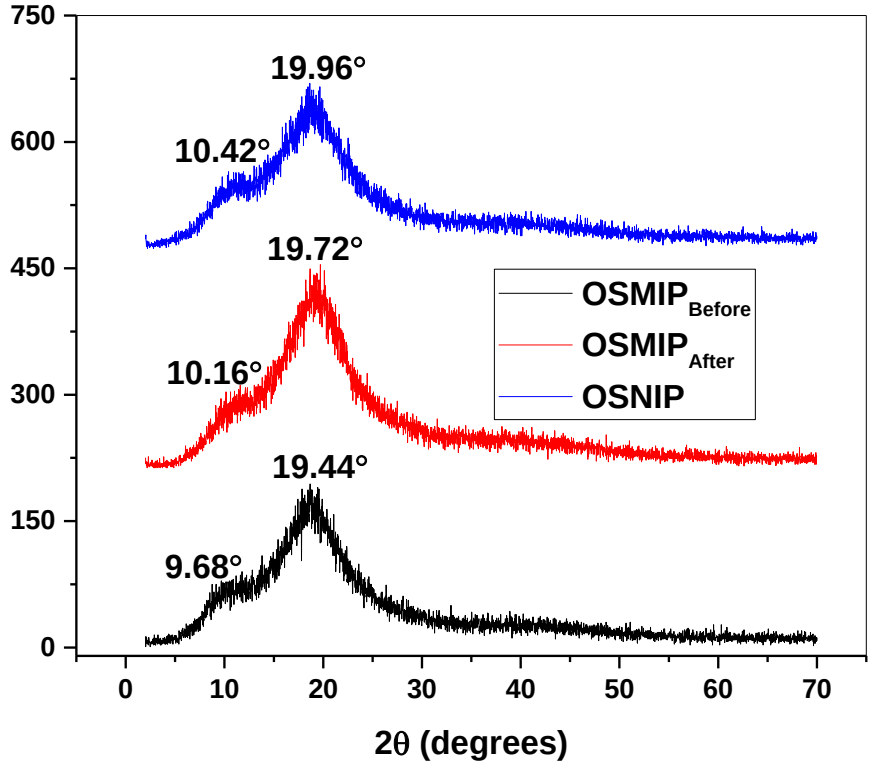

Figure 4: X-ray diffraction patterns of the polymers.

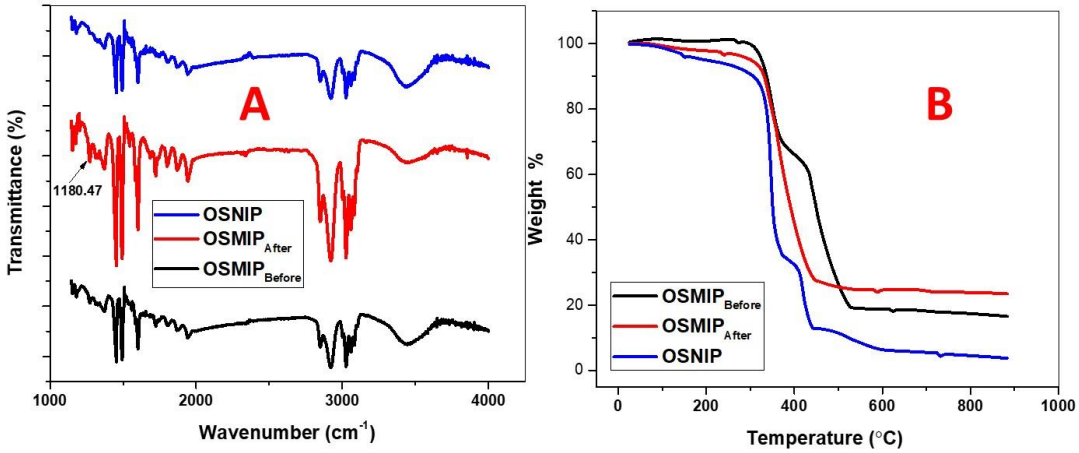

Figure 5: (A) Fourier Transform Infrared spectra and (B) Thermogravimetric analysis curves of the polymers

3.2. **Impact of pH, contact duration, and adsorption kinetics**

The pH of a solution plays a pivotal role in an adsorption process. It affects the overall charges involved in the interactions between the sorbate and the sorbent (Kubheka *et al.*, 2022). The role played by pH on the removal of BCGD by onion-skin based imprinted adsorbent from an

aqueous solution was tested across a pH range of 3 to 9 (Fig. 5A). The results indicate a lack of significant variation in BCGD elimination across the entire pH range, with the removal percentage consistently between 97.8 and 98.5% for $OSMIP$ and 60.1 and 62% for OSNIP. This suggests that neither H^+ nor OH^- ions significantly impact BCGD adsorption on the adsorbent. Therefore, the original pH of the BCGD solution, approximately 6.0, was maintained for the entire adsorption study.

The effect of contact time on adsorption of BCGD onto OSMIP and OSNIP were measured at an initial dye concentration of 50 mg L^{-1} and at seven different time range from 5 to 120 minutes are shown in Fig. 5B. Two major stages were apparently noted during the BCGD adsorption process. The first stage was rapid, with over 97% of the dye removed within approximately 15 min for OSMIP and 42% for OSNIP. Whilst the second stage was after 30 min that slowly increased to reach the equilibrium state in 60 min, indicating that BCGD molecule may be uniformly distributed across the OSMIP/OSNIP surface. Based on the profiles depicted in Fig. 5B, after 60 minutes of contact, the removal efficiencies for BCGD were approximately 54.1% for OSNIP and 98.7% for OSMIP. The noticeable contact time of 60 min was then set as the optimal duration to investigate the remaining operational parameters.

Upon examining the kinetic parameters data obtained from the four kinetic models as presented in Table 1, it is evident that deviation from the straight line were observed for the correlation coefficients (R^2) of the PFO and W-M models. The Elovich model was deemed to some extent suitable for fitting the experimental data considering the resulting R^2 values ranging between $0.9024 - 0.9113$. Thus, suggesting the involvement of chemisorption mechanism because Elovich model primarily depicts chemisorption process (Tan *et al.,* 2017; Awokoya *et al.,* 2024). In all the analyzed kinetic models, both in terms of adsorption capacities (q_e) and R^2, PSO kinetic model can be seen as providing the best fit having $R^2 = 1.0000\ and\ 0.9999$ for OSMIP and OSNIP, respectively. In addition, the q_e calculated values were found to closely matched the experimental values, which further strongly confirms that the PSO model most accurately defines the adsorption process of BCGD. In summary, chemisorption appears to be the predominant diffusion-rate-limiting step among the interactions involving BCGD and the functional groups of the imprinted adsorbent (Vimonses *et al.,* 2009). This finding aligns with parallel findings reported in the literature (Radoor *et al.,* 2021; Mamman, *et al.,* 2021).

3.3. **Influence of initial dye concentration and adsorption isotherms**

Figure 6C illustrates the impact of the initial dye concentration on the removal of BCGD. As the initial dye concentration rose from 25 to 200 mg/L, dye adsorption decreased from 99.8 to 97.1% for OSMIP and from 60.4 to 13.3% for OSNIP. This trend suggests a reduction in available binding sites (cavities) for further binding at higher concentrations. Furthermore, the high removal efficiency at low BCGD concentrations could also be due to enhanced interaction between dye molecules and the active sites within the adsorbent surface (Boubaker *et al.,* 2021). It is clear that OSMIP exhibited higher adsorption performance compared to OSNIP, for example, at 200 mg/L the removal efficiency for OSMIP (97.1%) was almost 7.3 times higher than that of OSNIP (13.3%). This high performance of OSMIP could be ascribed to the cavities imprinted on the polymer surface. Notably, the BCGD adsorption efficiency of OSMIP

adsorbent exhibited less sensitivity to variations in the initial adsorbate concentration compared to OSNIP. Similar results were obtained by Jinendra *et al.*, 2021 and Puchongkawarin *et al.*, 2021.

The adsorption equilibrium data were modeled using the Langmuir, Temkin, Dubinin-Radushkevich (D-R), and Freundlich equations, and the findings are presented in Table 2. Adsorption isotherms give information about the interactions between adsorbates and adsorbents, thus, predicting the specific nature of the interactions (Raval *et al.*, 2016). In comparison with three other isothermal models, Langmuir isotherm best fit the BCGD uptake data, suggesting monolayer BCGD coverage and energetically uniform adsorption sites on the adsorbents. This assertion is supported by the observed excellent correlation coefficient ($R^2 = 0.9322$ for OSMIP and $R^2 = 0.9365$ for OSNIP). Unfavorable correlation coefficients were observed when the data were modeled using the Dubinin-Radushkevich (D-R), Freundlich, Temkin, and isotherm models; therefore, these models seem to be less effective in representing experimental BCGD uptake data. For the D-R model, the free mean energy (E) values were found to be 12.41 and 11.11 $kJ\ mol^{-1}$ ($> 8\ kJ\ mol^{-1}$) for OSMIP and OSNIP, respectively, suggesting probable involvement of chemisorption process. Notably, the maximum adsorption capacity (q_{max}) of BCGD by the imprinted OSMIP was predicted to be 86.96 mg/g, which is significantly higher than those previously reported in the literature as presented in Table 3.

3.4. **Effect of temperature and thermodynamics modelling**

Temperature plays a crucial role in adsorption studies. Assessing the effect of temperature on the efficiency of the adsorption process is essential for any analysis (Corda and Kini, 2018). The adsorption of dye on OSMIP and OSNIP was examined over a temperature range of $303 - 333\ K$. As illustrated in Figure 6D, the adsorption limit and effectiveness for BCGD decrease as the temperature rises. This observation indicates that higher temperatures hinder the adsorption process, suggesting it is an exothermic process. Three basic thermodynamic parameters ΔG°, ΔS°, and ΔH° were studied (Table 4). The adsorption was determined to be exothermic, as indicated by the ΔH° negative values for both adsorbents, which was evaluated from the slope of ln K plotted against the inverse of temperature. This assertion aligns with the observations obtained from the effect temperature on BCGD adsorption. The negative ΔS° values showed that the adsorption process was driven by enthalpy towards spontaneity (Cestari *et al.*, 2006). The increase in ΔG° from -12.35 to -9.41 kJ mol^{-1} for OSMIP and -1.27 to 1.07 kJ mol^{-1} for OSNIP with rising temperature suggests an increased efficiency at higher temperatures, attributed to the increased mobility of BCGD molecule towards the adsorbent surface (Adebayo *et al.*, 2019). Overall, the negative values of ΔG° for OSMIP signify that the adsorption of dye by the imprinted polymer was both favorable and spontaneous across various temperatures. In contrast, for OSNIP, values of ΔG° were negative at 303 and 313 K, but changed at 323 and 333 K, thus suggesting a shift in the degree of randomness as the temperature increased. These findings are consistent with previous studies on the adsorption of malachite green and bromocresol green dyes (Awokoya *et al.*, 2024).

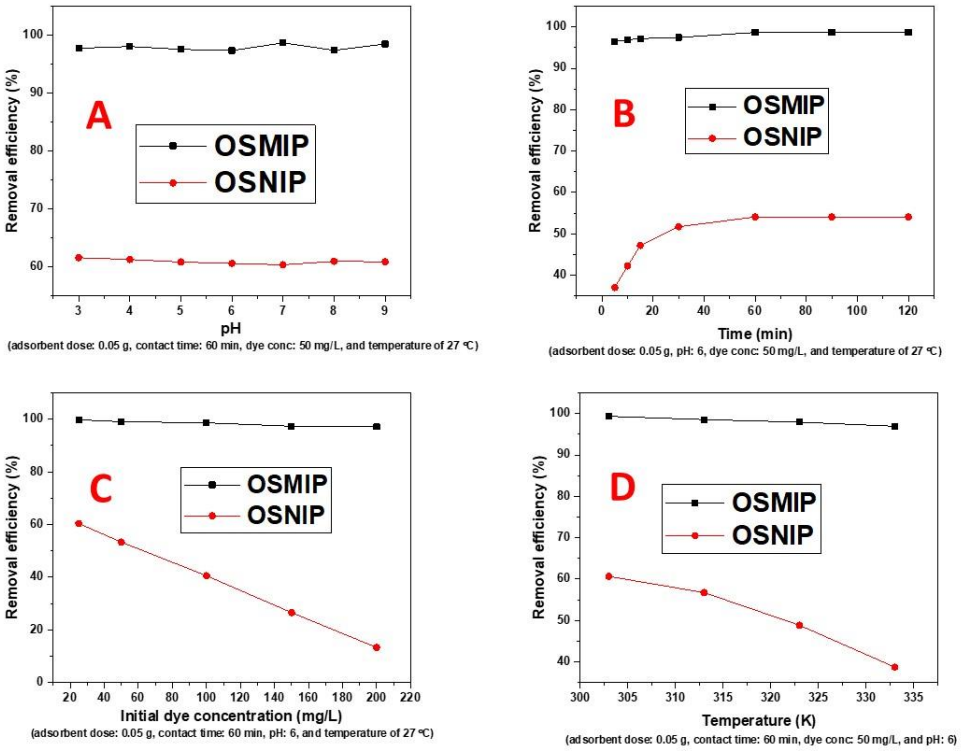

Figure 6: Effects of different operational parameters: (A) pH, (B) contact time (C) initial dye concentration and, (D) temperature on BCGD removal by OSMIP/OSNIP

Table 1: Linearized kinetic parameters for the adsorption of BCGD on OSMIP/OSNIP

Model	Parameter	OSMIP	OSNIP	Definition
PFO	R^2	0.8443	0.8355	q_t: amount of dye adsorbed
	k_1 (L/min)	0.0231	0.0399	k_1: PFO rate constant
	$q_{e(exp)}$ (mg/g)	0.1926	0.9476	
	$q_{e(calc)}$ (mg/g)	8.114	9.338	
PSO				
	R^2	1.0000	0.9999	
	k_2 (g/mg. min)	0.5045	0.0902	K_2: PSO rate constant
	$q_{e(exp)}$ (mg/g)	7.9177	4.4425	
	$q_{e(calc)}$ (mg/g)	7.8246	4.3678	
W-M	R^2	0.6612	0.6029	k_α: W-M rate constant
	k_α (mg/g. $min^{½}$)	0.0344	0.0213	C: intercept
	C	12.001	9.222	
Elovich				
	R^2	0.9113	0.9024	α: initial adsorption rate
	α (mg/g. min)	1.3 E+73	1.9E+115	β: desorption constant
	β	10.101	21.352	

Table 2: Temkin, Langmuir, Dubinin-Radushkevich, and Freundlich constants for the adsorption of BCGD onto OSMIP and OSNIP

Isotherm	Parameter	OSMIP	OSNIP	Definition
Langmuir	R^2	0.9322	0.9365	q_{max}: maximum dye adsorbed
	k_L (L/mg)	0.7931	-0.3678	K_L: Langmuir constant
	q_{max} (mg/g)	86.957	11.574	
Freundlich				
	R^2	0.8941	0.5873	k_F: Freundlich constants
	k_F (L/mg)	32.847	4.845	n: heterogeneity factor
	1/n	0.445	0.209	
D-R	R^2	0.7711	0.4589	β (mol^2/kJ^2): D-R constant
	q_m (mmol/g)	2 E+3	18.14	R (8.314 J/mol. K): gas constant
	E (kJ/mol)	12.41	11.11	ε (J/mol): Polanyi potential
				q_m: maximum dye adsorbed
				T (K): Temperature
				E: Energy
Temkin	R^2	0.4222	0.4449	B= RT/b: Temkin constant
	K_T(L/g)	5.0134	0.2376	
	b (kJ/mol)	10.13	27.88	K_T : Temkin adsorption potential

Table 3: Comparison of maximum adsorption capacity of BCGD on *OSMIP* with selected adsorbents

Adsorbent materials	Dose (g)	$Conc\ (mg\ L^{-1})$	$q_{max}\ (mg\ g^{-1})$	Reference
			BCGD	
This study	0.05	$25-200$	86.96	
Graphene oxide	*0.02*	25	16.83	(Robati *et al.* 2016)
White clove stem powder	*0.2*	50	1.95	(Gul *et al*. 2023)
Red seaweed powder	$0.25-0.3$	$5-40$	52.60	(Al-Saeedi *et al.* 2023)
Amorphous CNTs	$-$	$3.27-4.79$	21.51	(Banerjee *et al*. 2017)

Table 4: The Thermodynamic Parameters estimated for BCGD adsorption onto OSMIP and OSNIP

Adsorbent	ΔH (kJ/mol)	ΔS (kJ/mol.K)	ΔG			
			303 K	313 K	323 K	333 K
OSMIP	-42.034	-0.0979	-12.35	-11.37	-10.39	-9.41
OSNIP	-24.875	-0.0779	-1.27	-0.49	0.29	1.07

3.5. Regeneration and reusability

In this study, the regeneration of OSMIP adsorbent was carried out to regenerate the used polymer, lower production costs, reduce waste disposal expenses, and minimize the generation of secondary pollution. To determine the desorption efficiency, MeOH, and acetic acid were used as eluents, following a method previously reported by Awokoya *et al*. (2024). The reusability results of the OSMIP, shown in Figure 7, indicated that the adsorption efficiency of BCGD remained largely stable over the initial seven cycles (about 99.8%). Significant decreases in the adsorption capacity of the OSMIP were observed starting from the eight cycles (96.3%). This decline could be attributed to the occupation of adsorption sites by BCGD dye molecules and potential weakening of the functional groups on the OSMIP surface during regeneration. Overall, the results indicate a decline in OSMIP's adsorption effectiveness, dropping from 99.8 to 92.4% after ten consecutive recycling cycles.

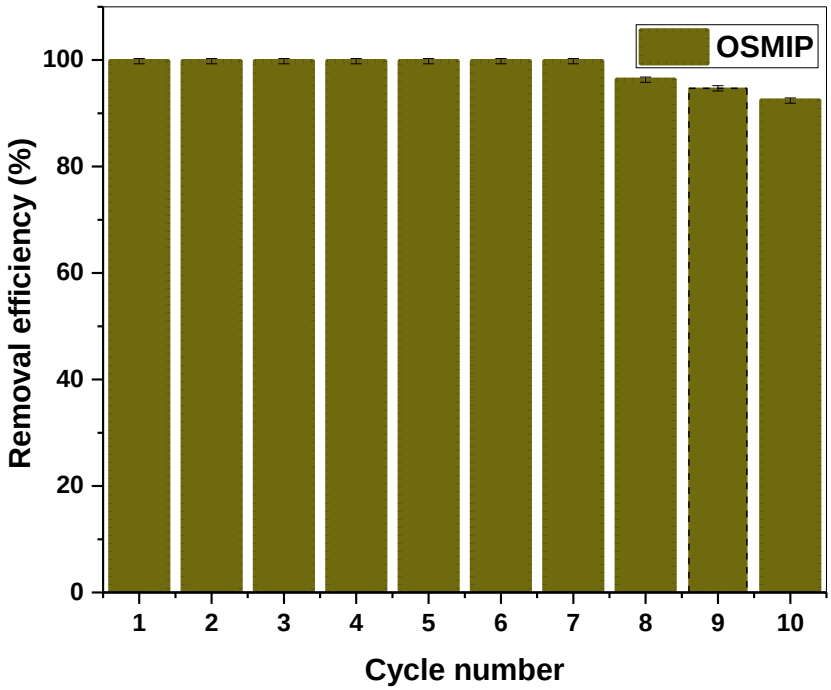

Figure 7: Reusability study of OSMIP towards BCGD adsorption

3.6. Use of polymer adsorbent for real environmental sample

To assess the effectiveness of the polymer adsorbent in removing BCGD from real environmental water sample, OSMIP was tested on a textile wastewater sample obtained from Ile-Ife City, Nigeria. A removal efficiency of approximately 84.78% was achieved for the BCGD molecule. Comparing the amount of BCGD adsorbed onto the OSMIP adsorbent in environmental sample with that in model water revealed that the removal efficiency in real textile sample is slightly lower than that observed in synthetic models. The data indicated that OSMIP is a cost-effective material with outstanding removal efficiency for treating wastewater containing BCGD in real textile wastewater samples.

3.7. Quantum chemical studies

The optimized structures of the pre-polymerization complexes at both HOMO and LUMO energy levels, as well as the DFT electronic parameters are presented in Figure 8 and Table 5, respectively. From Table 5, it could be seen that the complex of BCGD with styrene functional monomer
($BCGD - ST$) was the most stable with energy gap (ΔE) of 4.78 eV compared to the $BCGD - DVB$ complex having $\Delta E = 1.81\ eV$. Thus, styrene was chosen ahead of divinyl benzene as functional monomer in the synthetic procedure of this present study.

The η, μ and ΔN quantum descriptors are chemical parameters that perform significant and fundamental roles in predicting adsorption synergy interactions between the polymers (adsorbents) and BCGD analyte (adsorbates) (Awokoya *et al.,* 2022; Khnifira *et al*., 2022). As for the number of transferred electrons greater than zero ($\Delta N > 0$), this is an indication that there is strong tendency that the adhesion sites of the imprinted adsorbent could have been responsible for the electron's donation to the BCGD molecule (Obot *et al*., 2015).

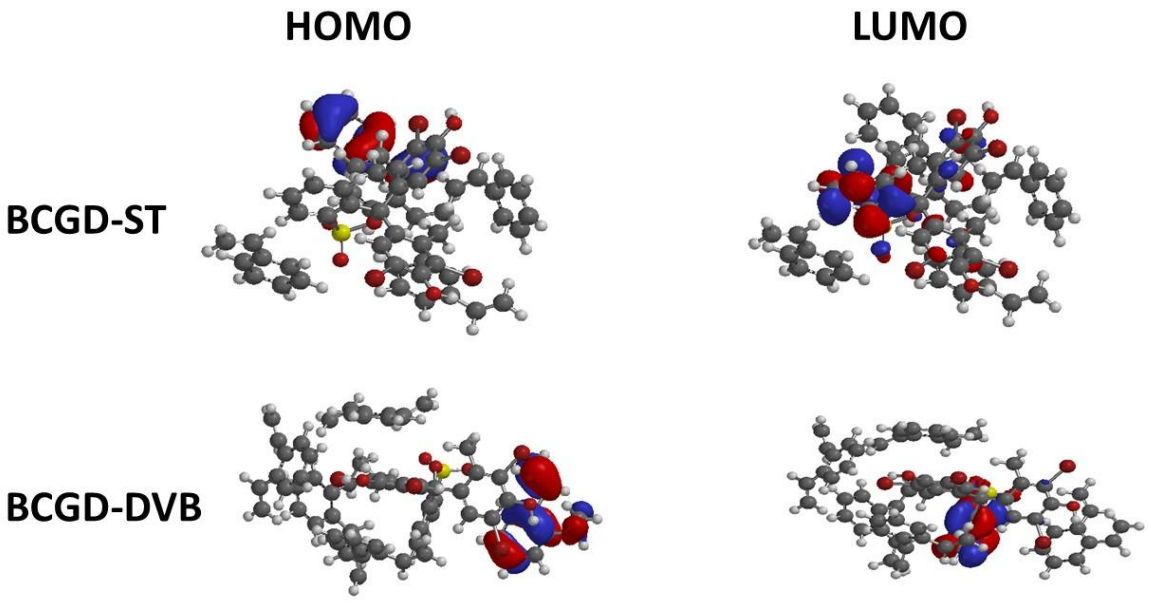

Figure 8: HOMO and LUMO molecular orbitals complexes between BCGD and styrene (BCGD-ST) and divinyl benzene (BCGD-DVB).

Table 5: Estimated DFT quantum electronic parameters

Compounds	E (eV)	E_{HOMO} (eV)	E_{LUMO} (eV)	ΔE	η	μ	ΔN
$Styrene\ (ST)$	-7314.81	-5.11	-0.52	4.4	2.46	-3.17	
$Divinylbenzene\ (DVB)$	-10531.9	-6.07	-0.83	5.24	2.62	-3.45	
$Bromocresol\ green\ (BCGD)$	-323228	-6.51	-1.58	4.93	2.465	-4.045	0.93
$BCGD - ST$	-365358	-6.04	-1.39	4.78	2.325	-3.715	
$BCGD - DVB$	-375888	-5.76	-1.39	1.81	2.185	-3.575	

4. Conclusions

The incorporation of onion skin, a natural material, into synthetic imprinted polymer for utilization as adsorbent in the removal of BCGD was studied. The successful synthesis of the onion skin-based molecularly imprinted polymer (OSMIP) was confirmed using various techniques, including XRD, FTIR, SEM-EDX, and TGA. The BCGD molecule–imprinted polymer (OSMIP) demonstrated both high efficiency and selectivity towards BCGD rebinding. For the dye removal experiment, several variables affecting adsorption efficiency were investigated for their influences on BCGD sequestration. Optimal adsorption time was established after 60 min of BCGD – OSMIP contact and at pH 6, with an adsorbent dose of 50 mg and analyte concentration of 50 mg L^{-1}. The pseudo-second-order model provided the best fit for the kinetic results with R^2 values ranging from 0.9999 to 1.0000. The data also fitted, to a large extent, well to the Elovich model, with R^2 values between 0.9024 and 0.9113. The Langmuir isotherm model best described the adsorption equilibrium data, with R^2 values from 0.9322 to 0.9365, indicating a monolayer BCGD coverage and energetically uniform adsorption sites on the adsorbents. Thermodynamic study showed that the adsorption process was exothermic, spontaneous, and driven by enthalpy. The OSMIP was used in ten consecutive cycles of adsorption and desorption, exhibiting a minimal loss in removal efficiency of just 7.4%. Density functional theory calculations suggested a strong likelihood that the adhesion sites of the OSMIP were responsible for donating electrons to the BCGD molecule. Thus, owing to its exceptional adsorption performance, OSMIP can be regarded as a highly effective and viable adsorbent for BCGD removal in aqueous medium.

Acknowledgements

The authors express their gratitude to the Polymer Science and Biophysical Chemistry Laboratory, Obafemi Awolowo University, Ile-Ife, Nigeria, for granting access to their facilities.

Funding and/or Conflicts of interests/Competing interests

We affirm that this manuscript has no known conflicts of interest, has not received funding from any source, and has no competing interests.

References

Adebayo, G.B., Jamiu, W., Okoro, H.K., Okeola, F.O., Adesina, A.K. and Feyisetan, O.A. (2019): Kinetics, thermodynamics and isothermal modelling of liquid phase adsorption of methylene blue onto moringa pod husk activated carbon. *S. Afr. J. Chem.*, 72, 263–273.

Adeola, A.O., Oyedotun, K.O., Waleng, N.J., Mamba, B.B. and Nomngongo, P.N. (2023): Onion skin–derived sorbent for the sequestration of methylparaben in contaminated aqueous medium. *Biomass Conv. Bioref.* https://doi.org/10.1007/s13399-023-04332-4.

Ali, I., Khan, T.A. and Hussain, I. (2011): Treatment and remediation methods for arsenic removal from the ground water. *International Journal of Environmental Engineering* 3, 48–71.

Al-Saeedi, S. I., Ashour, M. and Alprol, A. E. (2023): Adsorption of toxic dye using red seaweeds from synthetic aqueous solution and its application to industrial wastewater effluents. *Front. Mar. Sci.*, 10, 1202362. https://doi.org/10.3389/FMARS.2023.1202362/BIBTEX

Amel, K., Meniai, A. and Kerroum, D. (2012): Isotherm and Kinetics Study of Biosorption of Cationic Dye onto Banana Peel. *Energy Procedia* 19, 286–295.

Awokoya, K. N., Oninla, V. O., Adeyinka, G. C., Ajadi, M. O., Chidimma, O. T., Fakola, E. G. and Akinyele, O. F. (2022): Experimental and computational studies of microwave-assisted watermelon rind–styrene based molecular imprinted polymer for the removal of malachite green from aqueous solution. *Scientific African, 16*, e01194. DOI:10.1016/j.sciaf.2022.e01194

Awokoya, K. N., Oninla, V. O., Ogunkunle, O. A., Oyebode, B. A., Owoade, O. J., Obitusin, O. O.and Ipadeola, D.T. (2024): Preparation of styrene-based imprinted polymer for the adsorption of hazardous bromocresol green dye: equilibrium, kinetics and thermodynamics study. *Ife Journal of Science* 26, 45-57. https://dx.doi.org/10.4314/ijs.v26i1.4.

Awokoya, K.N., Batlokwa, B.S., Moronkola, B.A., Chigome, S., Ondigo, D.A., Tshentu, Z. and Torto, N. (2013): Development of a styrene based molecularly imprinted polymer and its molecular recognition properties of vanadyl tetraphenylporphyrin in organic media. *Inter J Polym Mat & Polym Biomater.*, 63, 107–113. https://dx.doi.org/10.1080/00914037.2013.769255

Awokoya, K.N., Oninla, V.O., Eugene-Osoikhia, T.T., Njionye, U.O., Okoya, A.A., Adeyinka, G.C. and Odor, C. (2024): Synthesis of trimethoprim vanillin anchored conjugate imprinted polymers for removal of bromocresol green and malachite green from aqueous media. *Water Science and Engineering*, https://doi.org/10.1016/j.wse.2024.01.004.

Babu, B.R., Parande, A.K., Raghu, S. and Kumar, T.P. (2007): Textile technology. Cotton textile processing: Waste generation and effluent treatment. *Journal of Cotton Science* 11, 141–153.

Banat, M.E., Nigam, P., Singh, D. and Marchant, R. (1996): Microbial decolourization of textile dye containing effluents, a review. *Biores. Technol.,* 58, 217-227. doi:10.1016/s0960-8524(96)00113-7.

Banerjee, D., Bhowmick, P., Pahari, D., Santra, S., Sarkar, S., Das, B. and Chattopadhyay, K. (2017): Pseudo first ordered adsorption of noxious textile dyes by low-temperature synthesized amorphous carbon nanotubes. *Physica E* 87, 68–76.

Boubaker, H., Ben Arfi, R., Mougin, K., Vaulot, C., Hajjar, S., Kunneman, P., Schrodj, G. and Ghorbal, A. (2021): New optimization approach for successive cationic and anionic dyes uptake using reed-based beads. *J. Cleaner Prod.,* 307, 127218.

Cestari, A.R., Vieira, E.F.S. and Mattos, C.R.S. (2006): Thermodynamics of the Cu (II) adsorption on thin vanillin-modified chitosan membranes. *The Journal of Chemical Thermodynamics* 38, 1092-1099.

Cheung, C.W., Porter, J.F. and McKay, G. (2000): Elovich equation and modified second-order equation for sorption of cadmium ions onto bone char. *Journal of Chemical Technology & Biotechnology* 75, 963-970. https://doi.org/10.1002/1097-4660(200011)75:11%3c963:AID-JCTB3 02%3e3.0.CO;2-Z.

Corda, N.C. and Kini, M.S. (2018): A review on adsorption of cationic dyes using activated carbon. *MATEC Web Conf.* 144, 1–16. (doi:10.1051/matecconf/ 201814402022).

Dubinin, M.M., Zaverina, E. and Radushkevich, L. (1947): Sorption and structure of active carbons. I. Adsorption of organic vapors. *Zhurnal Fizicheskoi Khimii 21*, 151-162.

Emembolu, L.N., Nwabanne, J.T. and Onu, C.E. (2017): Kinetic modeling of anaerobic digestion of restaurant waste water. *Br. J. Appl. Sci. Technol*., 21, 1 - 12. 10.9734/BJAST/2017/33397.

Fontana, I.B., Peterson, M. and Cechinel, M.A.P. (2018): Application of brewing waste as biosorbent for the removal of metallic ions present in groundwater and surface waters from coal regions. *J. Environ. Chem. Eng.,* 6, 660–670.

Freundlich, H. (1907): Über die adsorption in lösungen. *Zeitschrift für physikalische Chemie* 57, 385-470.

Gul, S., Afsar, S., Gul, H. and Ali, B. (2023): Removal of crystal violet dye from wastewater using low-cost biosorbent *Trifolium repens* stem powder. *J. Iran. Chem. Soc.*, 20, 2781-2792. https://doi.org/10.1007/S13738-023-02875-X/TABLES/3

Hai, F.I., Yamamoto, K. and Fukushi, K. (2007): Hybrid Treatment Systems for Dye Wastewater. *Crit. Rev. Environ. Sci. Technol*., 37, 315–377.

Hassan-Ibrahim, A. H., Cihangir, N., Idil, N. and Doruk Aracagök, Y. (2024): Adsorption of azo dye by biomass and immobilized Yarrowia lipolytica; equilibrium, kinetic and

thermodynamic studies. *World J Microbiol Biotechnol.*, 40, 140. https://doi.org/10.1007/s11274-024-03949-5.

Ho, Y.S. and McKay, G. (1999): Pseudo-second order model for sorption processes. *Process Biochemistry* 34, 451-465. doi.org/10.1016/S0032-9592(98)00112-5.

Holkar, C.R., Jadhav, A.J., Pinjari, D.V., Mahamuni, N.M. and Pandit, A.B. (2016): A critical review on Textile Wastewater treatments: possible approaches. J. Environ. Manag., 182, 351–366. doi: 10.1016/j.jenvman.2016.07.090.

Jain, A.K., Gupta, V.K., Bhatnagar, A. and Suhas, (2003): Utilization of industrial waste products as adsorbents for the removal of dyes. *Journal of Hazardous Materials*, 101, 31-42.

Jaramillo, C. M., Gutiérrez, T. J., Goyanes, S., Bernal, C. and Famà, L. (2016): Biodegradability and plasticizing effect of yerba mate extract on cassava starch edible films. *Carbohydrate Polymers*, 151, 150–159. https://doi.org/10.1016/j. carbpol.2016.05.025.

Jinendra, U., Nagabhushana, B.M. and Bilehal, D. (2021): Comparative adsorptive and kinetic study on the removal of malachite green in aqueous solution using titanium coated graphite and titanium coated graphite with Cnt-Abs nanocomposite. *Desalin. Water Treat.*, 209, 392–401.

Khajeh, M., Heidari, Z.S. and Sanchooli, E. (2011): Synthesis, characterization and removal of lead from water samples using lead-ion imprinted polymer. *Chem. Eng. J.*, 166, 1158–1163.

Khnifira, M., El Hamidi, S., Sadiq, M., Şimşek, S., Kaya, S., Barka, N. and Abdennouri, M. (2022): Adsorption mechanisms investigation of methylene blue on the (0 0 1) zeolite 4A surface in aqueous medium by computational approach and molecular dynamics. *Applied Surface Science*, 572, 151381. https://doi.org/10.1016/j.apsusc.2021.151381

Kubheka, G., Adeola, A.O. and Forbes, P.B.C. (2022): Hexadecylamine functionalised graphene quantum dots as suitable nano-adsorbents for phenanthrene removal from aqueous solution. *RSC Adv*., 12, 23922–23936. https://doi.org/10.1039/D2RA04641E

Kumar, P.S., Senthamarai, C. and Durgadevi, A. (2014): Adsorption kinetics, mechanism, isotherm, and thermodynamic analysis of copper ions onto the surface modified agricultural waste. *Environ. Prog. Sustain. Energy*, 33, 28–37.

Lagergren, S.K. (1898): About the theory of so-called adsorption of soluble substances. *Kungliga Svenska Vetenskapsakademiens Handlingar* 24, 1-39.

Langmuir, I. (1918): The adsorption of gases on plane surfaces of glass, mica and platinum. *Journal of the American Chemical society*, 40, 1361-1403. doi.org/10.1021/ja02242a004

Lellis, B., Fávaro-Polonio, C. Z., Pamphile, J. A. and Polonio, J. C. (2019): Effects of textile dyes on health and the environment and bioremediation potential of living organisms. *Biotechnol. Res. Innov.*, 3, 275-290.

Lu, Y., Wei, B., Wang, Y. and Li, J. (2007): Studies on the removal of bromocresol green from water by solvent sublation. *Sep. Sci. Technol.,* 42, 1901-1911. 10.1080/01496390601174398.

Mamman, S., Suah, F.B.M., Raaov, M., Mehamod, F.S., Asman, S. and Zain, N.N.M. (2021): Removal of bisphenol A from aqueous media using a highly selective adsorbent of hybridization cyclodextrin with magnetic molecularly imprinted polymer. *R. Soc. Open Sci.,* 8, 201604. https://doi.org/10.1098/rsos.201604

Matouq, M., Jildeh, N., Qtaishat, M., Hindiyeh, M. and Al Syouf, M.Q. (2015): The adsorption kinetics and modeling for heavy metals removal from wastewater by Moringa pods. *J. Environ. Chem. Eng*., 3, 775–784.

Mogren, L. (2006): Quercetin content in yellow onion (*Allium cepa L.)*: Effects of cultivation methods, curing and storage. Doctoral Thesis, Swedish University of Agricultural Sciences, Alnarp, Sweden.

Murmu, B.M., Behera, S.S., Das, S., Mohapatra, R.K, Bindhani, B.K. and Parhi, P.K. (2018): Extensive investigation on the study for the adsorption of bromocresol green (BCG) dye using activated Phragmites karka. *Indian J Chem Technol.,* 25, 409–420.

Nwabanne, J.T., Okpe, E.C., Asadu, C.C. and Onu, C.E. (2018): Sorption studies of dyestuffs on low-cost adsorbent. *Asian Journal of Physical and Chemical Sciences*, 5, 1–19.

Obot, I., Macdonald, D. and Gasem, Z. (2015): Density functional theory (DFT) as a powerful tool for designing new organic corrosion inhibitors: Part 1: an overview. *Corros. Sci*., 99, 1–30. doi.org/10.1016/j.corsci.2015.01.037.

Ogbodu, R.A., Omorogie, M.O., Unuabonah, E.I. and Babalola, J.O. (2015): Biosorption of heavy metals from aqueous solutions by Parkia biglobosa biomass: equilibrium, kinetics, and thermodynamic studies. *Environ. Prog. Sustain. Energy*, 34, 1694–1704.

Okan, O.L., Ugonabor, V.I., Onu, C.E. and Chinedu, J.U. (2022): Application of trickling filter with hybrid biofilm support media in the treatment of petroleum effluent. *LAUTECH J. Eng. Technol.,* 16, 94-105.

Prasad, C.V., Swamy, B.Y., Sudhakar, H., Sobharani, T., Sudhakar, K., Subha, M.C.S. and Rao, K.C. (2011). Preparation and characterization of 4A zeolite-flled mixed matrix membranes for pervaporation dehydration of isopropyl alcohol. *J Appl Polym Sci.,* 121, 1521–1529.

Puchongkawarin, C., Mattaraj, S. and Umpuch, C. (2021): Experimental and modeling studies of methylene blue adsorption onto Na-bentonite clay. *Eng Appl Sci Res.,* 48, 268–279.

Radoor, S., Karayil, J., Jayakumar, A., Parameswaranpillai, J. and Siengchin, S. (2021): An efficient removal of malachite green dye from aqueous environment using ZSM-5 zeolite/polyvinyl alcohol/carboxymethyl cellulose/sodium alginate bio composite. *Journal of Polymers and the Environment*, 29, 2126-2139.

Raval, N.P., Shah, P.U. and Shah, N.K. (2016). Nanoparticles loaded biopolymer as effective adsorbent for adsorptive removal of malachite green from aqueous solution. *Water Conserv Sci. Eng.* 1, 69–81.

Robati, D., Mirza, B., Rajabi, M., Moradi, O., Tyagi, I., Agarwal, S. and Gupta, V. (2016): Removal of hazardous dyes-BR 12 and methyl orange using graphene oxide as an adsorbent from aqueous phase. *Chem. Eng. J.*, 284, 687–697.

Seow, T.W., Lim, C.K., Nor, M.H.M., Mubarak, M.F.M., Lam, C.Y., Yahya, A. and Ibrahim, Z. (2016): Review on wastewater treatment technologies. Int. *J. Appl. Environ. Sci.*, 11, 111–126.

Tan, K. and Hameed, B. (2017): Insight into the adsorption kinetics models for the removal of contaminants from aqueous solutions. *J. Taiwan Inst. Chem. Eng*., 74, 25–48. doi.org/10.1016/j.jtice. 2017.01.024

Tempkin, M. and Pyzhev, V. (1940): Kinetics of ammonia synthesis on promoted iron catalyst. *Acta Phys. Chim. USSR,* 12, 327.

Trivedi, V.D., Saxena, I., Siddiqui, M.U. and Qasim, M.A. (1997): Interaction of bromocresol green with different serum albumins studied by fluorescence quenching. *Biochem. Mol. Biol. Int.* 43, 1–8.

Vimonses, V., Lei, S. and Jin, B. et al. (2009). Kinetic Study and Equilibrium Isotherm Analysis of Congo Red Adsorption by Clay Materials. *Chemical Engineering Journal*, 148, 354–364.

Wang, Y., Wei, H., Wang, Y., Peng, C. and Dai, J. (2021a): Chinese industrial water pollution and the prevention trends: An assessment based on environmental complaint reporting system (ECRS). *Alexandria Engineering Journal*, 60(6), 5803–5812. https://doi.org/10.1016/j.aej.2021.04.015.

Wang, X., Li, X., Peng, L., Han, S., Hao, C., Jiang, C., Wang, H. and Fan, X. (2021b): Effective Removal of Heavy Metals from Water Using Porous Lignin-Based Adsorbents. *Chemosphere*, 279, 130504.

Weber Jr, W.J. and Morris, J.C. (1963): Kinetics of adsorption on carbon from solution. Journal of the Sanitary Engineering Division 89: 31-59. doi.org/10.1061/JSEDAI.00004.

Yadav, A., Sharma, P., Panda, A.B., Shahi, V.K. (2021). Photocatalytic TiO2 incorporated PVDF-co-HFP UV-cleaning mixed matrix membranes for effective removal of dyes from synthetic wastewater system via membrane distillation. *J. Environ. Chem. Eng.*, 9, 1-12. 10.1016/j.jece.2021.105904.

Yang, Y., Li, X., Zhou, C., Xiong, W. and Zeng, G. (2020): Recent advances in application of graphitic carbon nitride-based catalysts for degrading organic contaminants in water through advanced oxidation processes beyond photocatalysis: A critical review. *Water Research*, 184. https://doi.org/10.1016/j.watres.2020.116200.

Yagub, M. T., Sen, T. K., Afroze, S. and Ang, H. M. (2014): Dye and its removal from aqueous solution by adsorption: A review. *Advances in Colloid and Interface Science,* 209, 172–184. https://doi.org/10.1016/j.cis.2014.04.002.

Zaharia, C., Diaconescu, R. and Surpăţeanu, M. (2007): Study of flocculation with Ponilit GT-2anionic polyelectrolyte applied into a chemical wastewater treatment. *Central European Journal of Chemistry*, 5, 239-256. doi:10.2478/s11532-006-0057-6.